

Volume behaviour of quark condensate, pion mass and decay constant from Dyson-Schwinger equations

Jan Luecker,¹ Christian S. Fischer,^{1,2} and Richard Williams¹

¹*Institut für Kernphysik, Technische Universität Darmstadt, Schlossgartenstraße 9,
D-64289 Darmstadt, Germany*

²*GSI Helmholtzzentrum für Schwerionenforschung GmbH,
Planckstr. 1 D-64291 Darmstadt, Germany.*

(Dated: May 5, 2021)

We solve the coupled system of Dyson-Schwinger and Bethe-Salpeter equations for the quark propagator and the pion Bethe-Salpeter amplitude on a finite volume. To this end we use a truncation scheme that includes pion cloud effects in the quark propagator and light mesons. We study volume effects in the quark condensate, the pion mass and the pion decay constant and compare to corresponding results in other approaches. In general we find large effects for volumes below $V = (1.8 \text{ fm})^4$.

PACS numbers: 12.38.Aw, 12.38.Gc, 12.38.Lg, 14.65.Bt

I. INTRODUCTION

Dynamical chiral symmetry breaking is one of the fundamental properties of QCD. Its pattern determines the experimentally observable spectrum of light hadrons as well as the details of the underlying interaction between quarks and gluons. It therefore plays a central role in our understanding of QCD. Despite great efforts in the last decades not all details of dynamical chiral symmetry breaking are as well understood as one could wish.

In this respect, the chiral properties of QCD at finite volume have attracted considerable attention over the years. Strictly speaking, dynamical chiral symmetry breaking and the associated formation of Goldstone bosons is restricted to the infinite volume limit. On any given finite volume the corresponding order parameter, the quark condensate $\langle \bar{q}q \rangle$, goes to zero in the limit of vanishing bare quark mass m . Nevertheless, one can extract the properties of the infinite volume theory from the formulation in a box. For large enough volumes and/or quark masses the box effects are small and the finite volume theory closely resembles its infinite volume limit. This happens if the condition

$$m V \langle \bar{q}q \rangle \gg 1, \quad (1)$$

is satisfied and the eigenvalues of the Dirac operator are almost dense [1]. On the other hand, if $m V \langle \bar{q}q \rangle \ll 1$ dynamical chiral symmetry breaking is lost.

Another important condition is the relation of the four-volume V with a typical hadronic scale Λ_H and the pseudo-Goldstone mass M_π . If the inequality

$$\frac{1}{\Lambda_H^4} \ll V \ll \frac{1}{M_\pi^4}, \quad (2)$$

is satisfied, the theory is in a critical region where long range correlations are at work. Here the

QCD partition function depends on the quark mass m and the volume only through the combination $\mu := m V \Sigma$, where Σ is the chiral condensate in the infinite volume limit. In this critical region exact, analytic and universal scaling laws are known from chiral random matrix theory [2–4], see *e.g.* [5] for a recent review. Certainly these are of great importance for approaches like lattice QCD which are inherently limited to finite volumes and lattice spacings.

The properties of QCD at finite volumes have been studied by several approaches. One, of course, is lattice QCD, see [6–11] and Refs. therein, but important insights have also been obtained from effective theories such as chiral perturbation theory [12–14], or the quark-meson model [15–17]. In this work we follow a complementary approach. We study volume effects in the quark condensate, the pion mass and the pion decay constant from the framework of Dyson-Schwinger equations (DSEs) of the quark propagator and the corresponding Bethe-Salpeter equations (BSEs) for pseudoscalar bound state amplitudes.

One of the advantages of this approach is that volume effects can be studied continuously from very small to very large volumes (corresponding studies for meson observables using chiral perturbation theory for example have to distinguish between two different regions of chiral counting). The implementation of mixed boundary conditions in the spatial and time directions is possible without great effort. Furthermore one has direct access to the infinite volume and the continuum limit without the need to perform any extrapolations. We are thus in a position to study chiral symmetry restoration at small volumes together with effects at large and infinite volumes in the same framework.

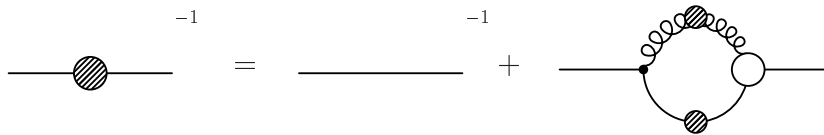


FIG. 1: The Dyson-Schwinger equation for the quark propagator. Filled circles denote dressed propagators whereas the empty circle stands for the dressed quark-gluon vertex.

On the other hand we need to work with a truncation scheme in order to close our system of equations. This scheme is systematic in the following sense: in a first step we neglect the volume dependence of the three-point functions. For the quark-gluon vertex we work with a volume independent ansatz that has proven useful in calculations of pion cloud effects in the masses of light mesons [18, 19]. The volume dependence of the gluon and quark propagators are then determined from their Dyson-Schwinger equations and serve as input into the volume dependent Bethe-Salpeter equation of the pion. This truncation scheme can be systematically extended to also include volume effects of higher Green's functions by explicitly solving their corresponding DSEs.

This work is organised as follows: In the next two subsections we summarise the properties of the quark Dyson-Schwinger equation and the Bethe-Salpeter equations on a torus. We then discuss details of the numerical treatment of these equations in subsection II C, whereas in subsection II D we specify our approximation scheme for the quark-gluon vertex. Our numerical results for the quark condensate are presented in section III A. We then proceed to discuss the volume dependence of the pion mass and decay constant in subsection III B. Starting with subsection III C we also take into account finite volume effects in the gluon propagator. We conclude and summarise in section IV.

II. QUARKS AND PIONS AT FINITE VOLUME

A. The quark Dyson-Schwinger equation on a torus

In Euclidean momentum space, the renormalised dressed gluon and quark propagators in the Landau gauge are given by

$$D_{\mu\nu}(p) = \left(\delta_{\mu\nu} - \frac{p_\mu p_\nu}{p^2} \right) \frac{Z(p^2)}{p^2}, \quad (3)$$

$$S(p) = \frac{1}{i\not{p}A(p^2) + B(p^2)}. \quad (4)$$

Here the gluon dressing function $Z(p^2)$ and the quark wave function $Z_f(p^2) = A^{-1}(p^2)$ also de-

pend on the renormalisation point, whereas the quark mass function $M(p^2) = B(p^2)/A(p^2)$ is a renormalisation group invariant. These propagators can be calculated from their Dyson-Schwinger equations (DSEs). Most important for this work is the DSE for the quark propagator which is shown diagrammatically in Fig. 1.

On a compact manifold, the gluon and quark fields have to obey appropriate boundary conditions in the time direction. These have to be periodic for the gluon fields and antiperiodic for the quarks. It is convenient, though not necessary, to choose the same conditions in the spatial directions. For the gluon propagator we will use periodic boundary conditions in all four space-time directions. For the quark field we will employ antiperiodic boundary conditions in all four directions. In principle it is also possible to implement periodic boundary conditions for the spatial directions of the quarks; corresponding results will be presented elsewhere.

We choose the box to be of equal length L in all spatial directions and a potentially longer value T in the time direction. The corresponding volume is denoted $V = T L^3$. Together with the boundary conditions the finite volume leads to discretised values in momentum space. Thus all momentum integrals appearing in the Dyson-Schwinger equations are replaced by sums over Matsubara modes. For the ghost and gluon DSE the corresponding equations as well as their solutions have been discussed in detail in Refs. [20–22]. The corresponding solutions in the infinite volume/continuum limit are given and discussed in Ref. [23]. To make this paper self-contained we shortly repeat the general features of these solutions below, where we discuss the quark-gluon interaction.

The quark-DSE on a torus has been discussed in Ref. [24, 25] at zero and in Ref. [26] at finite temperature, where results for the quark propagator and condensate at real quark momenta have been given. In the present work the quark propagator also serves as input into the Bethe-Salpeter equation for pseudoscalar mesons. As we will see this also necessitates the determination of the quark propagator for complex momenta.

Restricting our system to a finite volume results

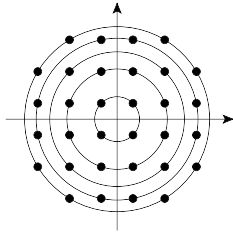


FIG. 2: The discretised momentum space that will be used: the momenta for antiperiodic boundary conditions in all directions. The circles indicate that only ‘full’ hyperspheres are taken into account, see text for details. This procedure leads to reduced cutoff effects.

in the Matsubara modes

$$p_i = \frac{2\pi}{L_i} n_i; \quad p_i = \frac{2\pi}{L_i} (n_i + 1/2) \quad (5)$$

for periodic and antiperiodic boundary conditions in direction i with length L_i and $n_i \in \mathbb{Z}$. With discretised momenta an integral in momentum space becomes

$$\int \frac{d^4 q}{(2\pi)^4} \rightarrow \frac{1}{L^3 T} \sum_{n_1, n_2, n_3, n_4 = -N}^{N_{max}}, \quad (6)$$

where N defines the maximal Matsubara mode, and therefore acts as an ultraviolet cutoff. Furthermore $N_{max} = N$ for periodic and $N_{max} = N - 1$ for

antiperiodic boundary conditions. Similar to the infinite volume case where one uses hyperspherical coordinates we rearrange the summation over Matsubara frequencies in the following convenient way

$$\sum_{n_1, n_2, n_3, n_4 = -N}^{N_{max}} = \sum_i \sum_m, \quad (7)$$

where i counts hyperspheres containing all momenta with the same absolute value and m counts individual momenta on each sphere. In the following we frequently use the notation

$$\sum_j := \sum_i \sum_m, \quad (8)$$

to account for the sum over all momenta q_j .

Fig. 2 shows how the discretised momentum space looks in two dimensions, with the circles indicating the hyperspheres that are counted by i . The hyperspheres that are not fully occupied for a given value of N are not used, *i.e.* hyperspheres that receive additional vectors when going from N to $N + 1$ are discarded. This procedure leads to an approximate restoration of rotational symmetry for large momenta. Consequently cutoff artefacts in the ultraviolet momentum regions are drastically reduced [20, 24, 27].

The Dyson-Schwinger equation for the quark propagator on a torus is then given by

$$S^{-1}(p_i) = Z_2 [S^0(p_i)]^{-1} - C_F \frac{Z_2}{\tilde{Z}_3} \frac{g^2}{L^3 T} \sum_j \gamma_\mu S(q_j) \Gamma_\nu(q_j, p_i) D_{\mu\nu}(p_i - q_j). \quad (9)$$

where the factor $C_F = 4/3$ stems from the colour trace and we have introduced a reduced quark-gluon vertex $\Gamma_\nu(q, p)$, by defining $\Gamma_{\nu,i}^{full}(q, p) = ig \frac{\lambda_i}{2} \Gamma_\nu(q, p)$. Here p and q denote the momenta of the two quark legs, whereas $k = p - q$ is the corresponding gluon momentum. The bare quark propagator is given by $[S^0(p)]^{-1} = i\gamma \cdot p + m(\Lambda^2)$, where $m(\Lambda^2)$ is the unrenormalised bare quark mass and Λ represents an ultraviolet cutoff. The wave function renormalisation factor Z_2 is determined in the renormalisation process. The ghost renormalisa-

tion factor \tilde{Z}_3 will be absorbed in our truncation of the quark-gluon vertex which we discuss below. The quark mass function $M(p^2)$ and the wave function $Z_f(p^2)$ can be extracted from Eq. (9) by suitable projections in Dirac-space.

B. The Bethe-Salpeter equation for the pion on a torus

The homogeneous Bethe-Salpeter equation (BSE) for flavour non-singlet mesons on a torus can be written as

$$\Gamma_{\alpha\beta}^\pi(p_i; P) = \frac{1}{L^3 T} \sum_j K_{\alpha\beta; \delta\gamma}(p_i, q_j; P) [S(q_j^+) \Gamma^\pi(q_j; P) S(q_j^-)]_{\gamma\delta} \quad (10)$$

where K is the Bethe-Salpeter kernel. The momenta $q^+ = q + \xi P$ and $q^- = q - (1 - \xi)P$ of the quark constituents are chosen such that the total meson momentum is given by $P = q^+ - q^-$. Here the momentum partitioning parameter $\xi = [0, 1]$ reflects the arbitrariness in the relative momenta of the quark-antiquark pair. Since all observables are independent of ξ we can choose $\xi = \frac{1}{2}$ without loss of generality. The flavour content of the meson is expressed through flavour matrices which are suppressed in Eq. (10). The Greek indices ($\alpha \dots$) refer to colour and Dirac structure. The BSE is a parametric eigenvalue equation with discrete solutions $P^2 = -M_n^2$ where M_n is the mass of the bound-state. The lowest mass solution corresponds to the physical ground state. Since P^2 is negative, the momenta q^\pm are necessarily complex in Euclidean space and so the quark propagator functions must be evaluated with complex argument. This leads to technical issues that are dealt with in subsection II C.

In general the pion Bethe-Salpeter amplitude can be decomposed into four different tensor structures $F_{1..4}$ according to

$$\Gamma^\pi(p_i; P) = \gamma_5 \left[F_1(p_i; P) - i \not{P} F_2(p_i; P) - i \not{p}_i (p_i \cdot P) F_3(p_i; P) - [\not{P}, \not{p}_i] F_4(p_i; P) \right]. \quad (11)$$

The specific values for the momenta p_i depend on our choice of boundary conditions for the quark fields. In the time direction the relative momenta p_i of the pion constituents have to be antiperiodic as can be seen from the exact expression [28]

$$F_1(p_i; P) = \frac{B(p_i)}{f_\pi}, \quad (12)$$

in the chiral limit, where B is the scalar quark dressing function and f_π the pion decay constant. With our choice of antiperiodic boundary conditions for the quark fields in all four direction we obtain the same boundary conditions for the p_i . The total momentum P of the pion is fixed by the condition $-P^2 = M_\pi^2$ on the momentum shell of the pion.

The (normalised) Bethe-Salpeter amplitudes of the pion Γ^π can be used to determine the pion decay constant according to

$$f_\pi = \frac{3Z_2}{M^2} \frac{1}{L^3 T} \sum_j \text{tr} [\Gamma^\pi(q_j, -P) S(q_j^+) \gamma_5 \not{P} S(q_j^-)] \quad (13)$$

on our torus. Here the trace is over Dirac matrices, and $q^\pm = q \pm P/2$. As for the normalisation condition for the pion amplitude we use a prescription originally proposed by Nakanishi in Ref. [29] and put to use for momentum dependent kernels in [30].

C. Solving the DSE for complex momenta

As we have seen, in the pion BSE the quark propagators are required for complex momenta

$$p^\pm = p \pm \frac{P}{2}, \quad (14)$$

in the rest frame $P = (0, 0, 0, iM_\pi)$ of the pion and real p . To evaluate the quark DSE at these complex arguments it is convenient to determine the quark dressing functions $A(p)$ and $B(p)$ as functions of p instead of the usual p^2 . Numerically we solve the quark DSE for fixed gluon propagator and quark-gluon vertex by a plain fixed point iteration method. This iteration has to be carried out on the grid of real parts p_j of p^\pm with fixed imaginary parts parametrised by M_π . Thus for any given value of M_π the quark DSE can be solved self-consistently without requiring knowledge of the propagator at a different M_π . Of course, due to symmetries it is not necessary to iterate the DSE for the full grid of momenta p_j^\pm but for a subset parametrised by the absolute value of the p_j , their four components $(p_j)_4$ and the pion momentum M_π .

When solving the quark DSE, Fig.1, in the complex plane one encounters the following ambiguity: since analytic continuation is not unique anymore on the discretised Matsubara frequencies one obtains results in the complex plane which are dependent on the momentum routing in the dressing loop of the DSE. This ambiguity is dependent on the volume. It is small for volumes larger than $V = (2 \text{ fm})^4$, *i.e.* in the region where volume effects are small anyhow. Below $V = (1.5 \text{ fm})^4$, however, there are sizeable effects. In this work we choose a momentum routing where the complex momentum goes through the quark part of the loop, whereas the gluon part depends on the real loop momentum only. Other choices probe the gluon propagator in the complex plane where no numerical results are available so far.

D. Truncation scheme for the quark-gluon interaction

We now proceed by specifying the explicit interaction used in the quark-DSE Eq. (9) and the BSE Eq. (10). It consists of two distinct parts, the dressed gluon propagator and the dressed quark-gluon vertex. For the gluon propagator we use solutions from the ghost and gluon DSEs as obtained in Refs. [22, 23]. There the system of DSEs has been solved using a specific truncation scheme for the ghost-gluon vertex and the three-gluon vertex as input. The resulting dressing functions for

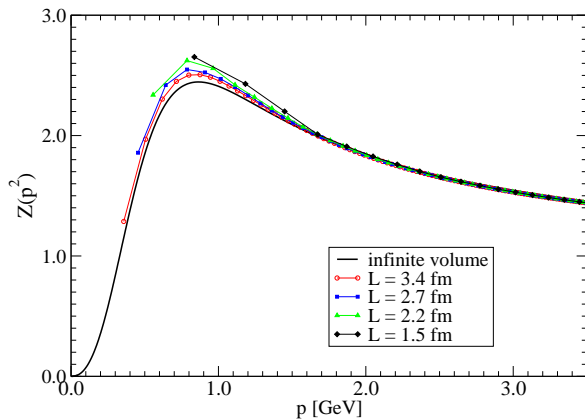


FIG. 3: Finite volume effects in the gluon dressing function $Z(p^2)$ as determined in Ref. [22].

the ghost and gluon propagator are in good qualitative agreement with corresponding lattice results with a quantitative difference of the order of ten percent at the peak of the gluon dressing function for momenta around $p = 1$ GeV. This is in marked contrast to corresponding dressing functions obtained from other approaches as *e.g.* the background gauge formalism [31], where there is almost an order of magnitude difference between the characteristic scale of the DSE-solution and the lattice result. Thus, the results of [31] cannot be used in phenomenological calculations as they would necessitate an artificially strong quark-gluon vertex in order to provide for enough interaction strength to generate dynamical chiral symmetry breaking.

In general, two types of solutions for the ghost and gluon propagators have been found in the deep infrared momentum region. There is a ‘scaling’ solution corresponding to an infrared vanishing gluon propagator and an infrared diverging ghost dressing function and there is a continuous family of ‘decoupling’ solutions corresponding to an infrared finite gluon propagator and an infrared finite ghost dressing function, see *e.g.* [23, 32, 33] and references therein. Recently, this family of decoupling solutions plus the limiting scaling one has been connected with ambiguities of fixing Landau gauge completely [34]. It is furthermore a current issue of intense debate whether and how these two solutions relate to important fundamental questions like the mechanism of confinement of QCD and the possibility of a nonperturbative BRST-symmetry. Fortunately for the purposes of this work the behaviour in the deep infrared is irrelevant since scaling vs. decoupling distinguishes the ghost and gluon at momentum scales below $p^2 = 50$ MeV² corresponding to volumes far larger than the ones investigated here.

For the gluon propagator at finite volume and discretisation we could in principle use results

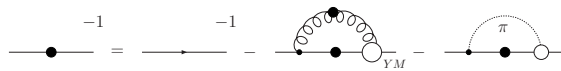


FIG. 4: The approximated Schwinger-Dyson equation for the quark propagator with effective one-gluon exchange and one-pion exchange.

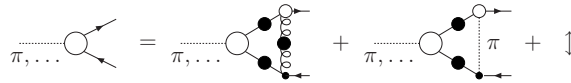


FIG. 5: The Bethe-Salpeter equation corresponding to the quark self-energy of Fig. 4. The up-down arrow indicates an averaging procedure of the pion exchange diagram with its counterpart where the upper pion-quark vertex is bare and the lower one dressed.

obtained on a torus [22], *cf.* Fig. 3. However, since corresponding results for the finite volume quark-gluon vertex are not yet available we believe it could be more systematic if we neglect volume effects in the gluon propagator as well. The numerical results in sections III A and III B are therefore obtained with the infinite volume/continuum gluon propagator evaluated at the bosonic Matsubara frequencies appearing in the quark DSE Eq. (9). Nevertheless we also performed some calculations including finite volume effects in the gluon propagator which are discussed in section III B.

Next we give an explicit expression for the quark-gluon vertex. Here we follow the strategy of Ref. [19] and split the vertex into a part containing only effects from pure Yang-Mills theory and a part containing the effects of pion backreactions to the quark propagator. The resulting interaction is given diagrammatically in figures 4 and 5. It satisfies the axial-vector Ward-Takahashi identity which is mandatory to obtain the pion as a Goldstone boson in the chiral and infinite volume limit.

The Yang-Mills part of the quark gluon vertex in this approximation is given by [19]

$$\Gamma_\nu^{YM}(k^2) = \gamma_\nu Z_2/\tilde{Z}_3 \Gamma^{YM}(k^2), \quad (15)$$

$$\begin{aligned} \Gamma^{YM}(k^2) &= \left(\frac{k^2}{k^2 + d_2} \right)^{-1/2-\kappa} \\ &\times \left(\frac{d_1}{d_2 + k^2} + \frac{k^2 d_3}{d_2^2 + (k^2 - d_2)^2} + \frac{k^2}{\Lambda_{\text{QCD}}^2 + k^2} \right. \\ &\times \left. \left[\frac{4\pi}{\beta_0 \alpha_\mu} \left(\frac{1}{\log\left(\frac{k^2}{\Lambda_{\text{QCD}}^2}\right)} - \frac{\Lambda_{\text{QCD}}^2}{k^2 - \Lambda_{\text{QCD}}^2} \right) \right]^{-2\delta} \right) \end{aligned} \quad (16)$$

with the gluon momentum k^2 , the one-loop value $\delta = \frac{-9N_c}{44N_c - 8N_f}$ for the anomalous dimension of the

re-summed ghost dressing function and $\alpha_\mu = 0.2$. We also use $\Lambda_{\text{QCD}}^2 = 0.52 \text{ GeV}^2$ similar to the scale obtained in Ref. [35]. The infrared exponent κ has been determined analytically in [36, 37] and is given by $\kappa = (93 - \sqrt{1201})/98 \simeq 0.595$. While Z_2 is determined selfconsistently in the quark-DSE we choose $\tilde{Z}_3 = 1$ for the ghost renormalisation factor. Since the combination of α_μ , the gluon dressing function and the two factors of $1/\tilde{Z}_3$ from the bare and dressed quark-gluon vertex together form a renormalisation group invariant this choice is possible without affecting multiplicative renormalisability of the quark-DSE. The only remaining free parameters of our interaction are d_1 , d_2 and d_3 . These have been determined in [19] to reproduce the physical pion mass and decay constant as well as a reasonable mass of the η' in the chiral limit [18]. The resulting choice is $d_1 = 1.45 \text{ GeV}^2$, $d_2 = 0.1 \text{ GeV}^2$ and $d_3 = 3.95 \text{ GeV}^2$.

The construction Eq. (15) follows the frequently used rainbow-ladder approximation of the full vertex and therefore involves only the γ_ν -part of its tensor structure. Note, however, that it has been shown in Ref. [38] that such a model cannot capture all essentials of dynamical chiral symmetry breaking. Nevertheless it represents a useful starting point for our investigation.

It remains to specify the quark meson vertex for the backreaction of the pion to the quarks. Here we employ only the leading part of the pion amplitude Eq. (11) given by the function $F_1(p_i; P)$. In Ref. [19] the chiral limit relation Eq. (12) has been used to represent the pion. However, since $B \equiv 0$ in the chiral limit on a torus this is not an option here. Instead we use the approximation

$$\Gamma^\pi(p_i; P) = \gamma_5 F_1(\Re(p_i^2), p_i \cdot P = 0, P^2) \quad (17)$$

where $\Re(p_i^2)$ is the real value of p_i^2 . Since F_1 is calculated from the volume dependent pion BSE this approximation takes volume effects in the pion wave function into account. As we will see, this model is elaborate enough to obtain a qualitative picture of volume effects due to the pion backreaction.

III. NUMERICAL RESULTS

Having discussed the details of our truncation for the quark-gluon interaction we now proceed to present our numerical results. All results shown are obtained using antiperiodic boundary conditions in all four space-time directions. We will also use $L = T$; other choices are possible in principle and will be dealt with elsewhere.

A. Volume and quark mass dependence of the quark condensate

Let us first discuss the volume and quark mass dependence of the quark condensate. With finite volume $V = L^3 T$ this quantity can be extracted from the dressed quark propagator via

$$\langle \bar{q}q \rangle = \frac{4Z_2 N_c}{L^3 T} \sum_j \frac{B(p_j^2)}{p_j^2 A^2(p_j^2) + B^2(p_j^2)}, \quad (18)$$

The result is a renormalisation point independent but cutoff dependent condensate. At finite bare quark masses, necessary in a finite volume, this quantity contains quadratic divergences in the continuum limit of infinite ultraviolet cutoff. Therefore in principle one has to think about the necessity of subtractions. However, it has been argued in Refs. [1, 7] that subtractions are not necessary in the finite volume scaling regime, *i.e.* in the region of volume and quark mass where the condensate is a function of the dimensionless variable $\mu = mV\Sigma$ only. Here Σ represents the chiral condensate in the infinite volume limit. In this region the ultraviolet divergences of the form $m\Lambda^2$ and $m^3 \ln \Lambda$ with cutoff Λ are suppressed by $1/V$ and $1/V^3$ respectively. These corrections are non-universal.

The leading behaviour of $\langle \bar{q}q \rangle(\mu)$, however, is universal in the scaling regime and can be calculated from random matrix theory (RMT) [5]. For quarks in the fundamental representation of $SU(3)$ gauge theory the result is given by

$$\frac{\langle \bar{q}q \rangle}{\Sigma} = \mu [I_{N_f+\nu}(\mu) K_{N_f+\nu}(\mu) + I_{N_f+\nu+1}(\mu) K_{N_f+\nu-1}(\mu)] \quad (19)$$

where the I_n and K_n are modified Bessel functions and ν is the topological charge.

In the following we determine the quark condensate in this scaling regime from solutions of our quark DSE for appropriate volumes and quark masses. We work in quenched approximation, *i.e.* $N_f = 0$. Our result is displayed in the left diagram of Fig. 6 together with RMT scaling according to Eq. (19). We clearly do observe scaling of the condensate with the dimensionless variable μ . However, the quantitative details of our results do not agree with the scaling behaviour predicted by RMT. So what is going wrong? The reason for this discrepancy can be explained from the limitations of our truncation scheme: of course one would expect to see RMT-scaling if and only if all Green's functions used in the quark-DSE would scale with μ . Unfortunately this is not the case for our volume and quark mass independent input, namely the gluon propagator and the dressed quark-gluon vertex. These quantities constitute a

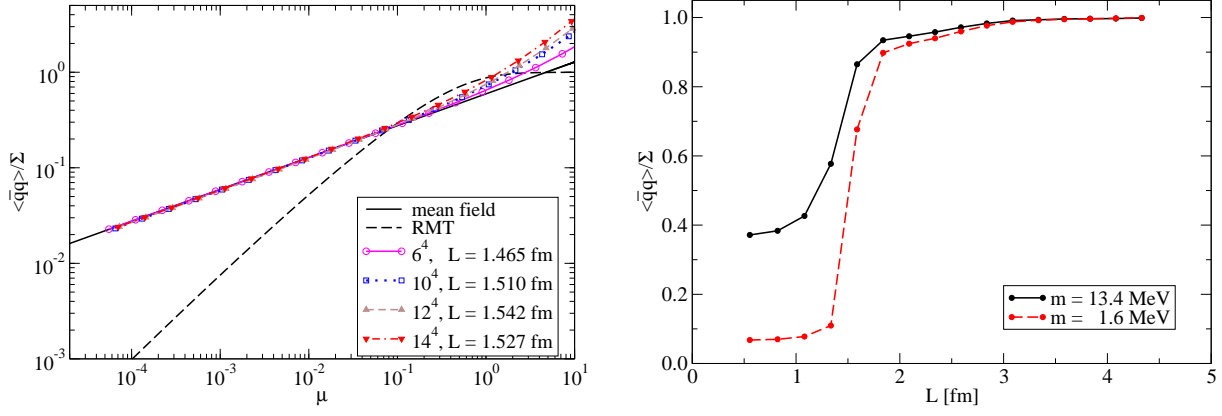


FIG. 6: Left diagram: The quark condensate $\langle \bar{q}q \rangle$ normalised by its infinite volume chiral value Σ as a function of the dimensionless variable $\mu = mV\Sigma$. Shown are mean field scaling and the result from random matrix theory compared to our results from the quark-DSE for several lattice sizes and box lengths. Right diagram: The quark condensate evaluated as a function of box length L for two different quark masses m corresponding to pion masses of $M_\pi = 100, 300$ MeV.

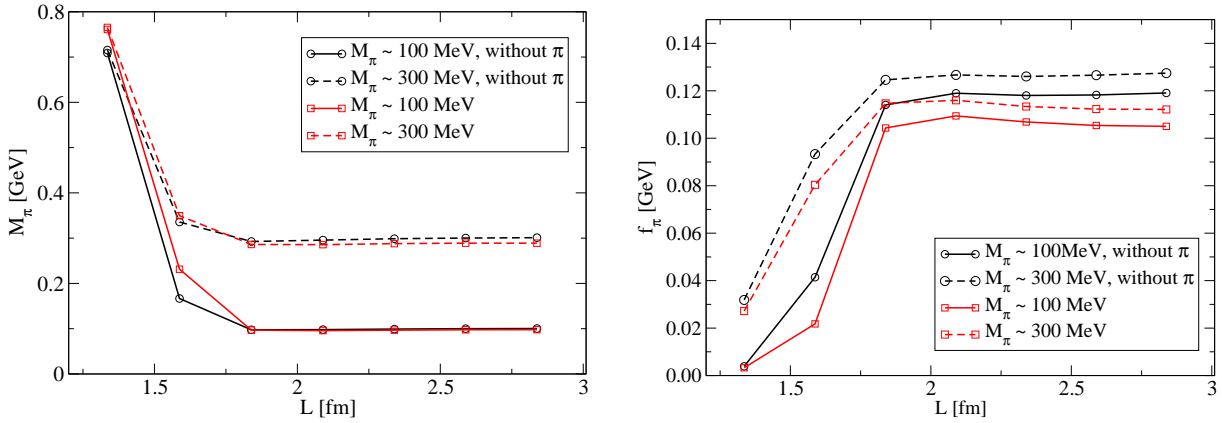


FIG. 7: Left diagram: The pion mass as a function of box length L for two different infinite volume pion masses once without ('without π ') and once including the pion backreaction to the quark propagator. Right diagram: Same as left diagram but for the pion decay constant.

μ -independent background in which the quark condensate is evaluated. Nevertheless the volume and quark mass effects associated with the quark-DSE Eq. (9) itself are present. As a result one should expect mean field scaling of the quark condensate as a function of μ :

$$\langle \bar{q}q \rangle(\mu) \sim \mu^{1/\delta}, \quad (20)$$

with $\delta = 3$. This is indeed what we observe. As can be seen from Fig. 6, in the scaling region $\mu \leq 1$ our result satisfies Eq. (20) with very good accuracy. We also observe critical slowing down in our numerics. We have checked that the scaling Eq. (20) persists in our solutions regardless of the details of the truncation of the quark-gluon vertex and also for different boundary conditions of the quark field. Around $\mu \sim 1$ the aforementioned cut-off effects set in and take over completely for $\mu > 10$. It will certainly be interesting to check whether

RMT-scaling appears in our approach when the restrictions on the quark-gluon vertex are lifted and volume and quark mass effects in the vertex are taken into account. This is, however, beyond the scope of the present work.

In the right hand diagram of Fig. 6 we also show the quark condensate evaluated as a function of box length for two different quark masses. Again we clearly observe that there is a critical region of volume below which the pattern of chiral symmetry breaking is changed substantially and finally lost for very small volumes [24, 25]. This happens roughly around $L = 1.5$ fm which is also the characteristic length scale for the mean field scaling we observe.

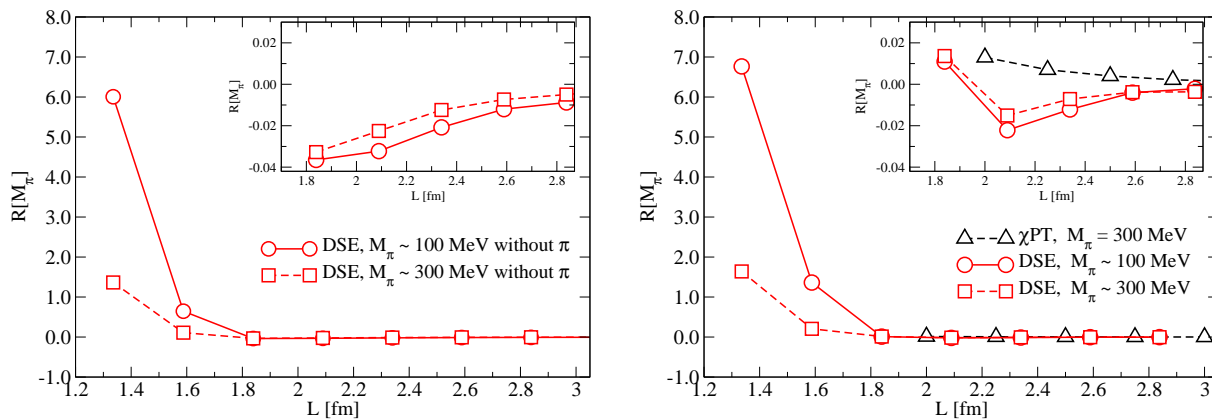


FIG. 8: The $R[M_\pi]$ ratio as a function of box length. Shown are our results for two different pion masses without (left diagram) and with the inclusion of pion cloud effects (right diagram). The latter results are compared to corresponding ones from chiral perturbation theory [13]. The inlays magnify the region where our results have a negative sign.

B. Volume and quark mass dependence of the pion mass and decay constant

In the previous section we discussed the volume dependence of a gauge invariant quantity, the quark condensate. Next we focus on two other gauge invariant quantities, the pion mass and the pion decay constant. In Fig. 7 we show our results for the volume dependence of these quantities. In order to also discuss effects due to different bare quark masses we include results corresponding to two different pion masses in the infinite volume limit, $M_\pi \approx 100, 300$ MeV. Furthermore in each diagram we show results with and without taking the pion backreaction to the quark propagator into account.

As concerns the pion mass, we see only very small effects for volumes larger than $V = (1.8\text{fm})^4$. These volumes seem to be large enough to be close to the infinite volume limit. For the pion decay constant, however, the situation is different: there are deviations from the infinite volume limit of the order of five percent up to volumes of $V = (2.3\text{fm})^4$. Recalling Eq. (13) we find that the calculation of f_π directly includes the pion wave function. On the other hand this quantity is absent in the rainbow-ladder calculation of the pion mass and only present at a subleading level when we additionally backcouple the pions to the quarks. Our result for $f_\pi(L)$ then indicates that volume effects in the wave function of the pion are larger than the ones in its pole mass. This is as expected from the general considerations of Ref. [1].

In Fig. 8 we present results for the quantity

$$R[M_\pi] = \frac{M_\pi(L) - M_\pi(\infty)}{M_\pi(\infty)} \quad (21)$$

which is sensitive to the deviation of the pion

mass in a box of length L compared to the infinite volume limit. In the left diagram we show results without the inclusion of the pion backreaction on the quark propagator, in the right diagram we show results taking these pion cloud effects into account. We study two different pion masses $M_\pi = 100, 300$ MeV. In general the size of the volume effects are larger for the smaller pion mass as expected. In both calculations we observe a positive shift of $R[M_\pi]$ if the box length is very small, followed by a turnover and a negative shift for box lengths larger than $L \approx 1.6 - 1.9$ fm. The negative shift is larger and sets in at smaller volumes if pion cloud effects are omitted (left diagram). Therefore it seems as if this negative shift may predominantly be a property of the quenched theory. Indeed, the very same sign change in the $R[M_\pi]$ -function has also been observed in quenched lattice QCD [8]. Our results without pion backreaction are therefore in qualitative agreement with the lattice results. In order to compare also quantitatively we would have to introduce periodic boundary conditions in the spatial directions as well as different box lengths in the space and time directions. This study is relegated to future work.

In the right diagram of Fig. 8 we compare our results (including pion cloud effects) with a corresponding one for the heavy pion extracted from a resummed form of Lüscher's formula together with input from chiral perturbation theory at next-to-next-to-leading order [13]. For the light pion the χPT -calculation is outside the range of applicability of the p -counting-regime and therefore not shown in the plot. For the heavy pion mass our results show the onset of volume effects at similar length scales than χPT , however the sign is different. χPT predicts a positive shift in $R[M_\pi]$ for all volumes. Since we have seen that our nega-

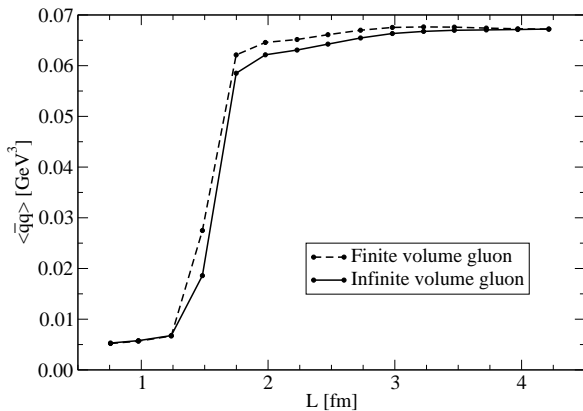


FIG. 9: The chiral condensate as a function of box length once calculated with and once without finite volume effects in the gluon propagator.

tive trend in $R[M_\pi]$ indeed gets smaller when we take the pion backreaction into account we can not exclude that our result even changes into the positive domain when we treat the pion cloud effects more systematically. This will be explored in future work. We wish to note, however, that negative values for $R[M_\pi]$ have also been observed in the quark meson model for unequal spatial and temporal box lengths, see [16, 17] for details.

C. Additional volume effects due the gluon

Finally we discuss additional volume effects in the chiral condensate due to volume effects in the gluon propagator. As discussed in section IID these effects should be included together with the corresponding effects in the quark-gluon vertex. Nevertheless it may be instructive to explore the size of the effects due to the gluon alone. For the quark mass function these have already been discussed in Ref. [24, 25]. Note that in [24] the volume effects in the gluon propagator have been overestimated and consequently unrealistically large effects in the quark mass have been found. This finding has been corrected in [25] using the updated calculation of the finite volume gluon propagator from [22]. Here we use a similar input, as detailed in section IID.

Our results are shown in Fig. 9. We clearly observe a similar qualitative behaviour with and without the finite volume gluon. The quantitative differences between the two calculations are small (*i.e.* below five percent) apart from a small region around $L = 1.5$ fm, where the vanishing of chiral effects happens at slightly different scales. For very small volumes both results become equal. This is easily understood since in this region the quark condensate is dominated from the bare quark mass

and dynamical effects are almost absent. We also performed calculations of the pion mass and decay constant using the finite volume gluon propagator and found even smaller effects there. Therefore we agree with the previous finding of [25]: the effect of finite volume corrections in the gluon propagator on physical observables is small.

IV. SUMMARY AND CONCLUSIONS

In this work we presented an exploratory study of volume effects in the quark condensate, the pion mass and its decay constant determined from a coupled set of Dyson-Schwinger (DSEs) and Bethe-Salpeter equations (BSEs). These equations are capable of connecting the large and small regions of momenta, quark masses and volumes, and therefore provide an interesting tool to determine these effects systematically. In our exploratory study we concentrated on volume effects generated in the quark DSE and the pion BSE and neglected corresponding effects in the quark-gluon vertex. This deficiency introduces a volume independent scale. Consequently, at small volumes we do not observe the universal scaling of the condensate as a function of $\mu = mV\Sigma$ predicted from random matrix theory. Instead we find critical scaling with mean field exponents at box lengths of $L \approx 1.5$ fm. In general we observe strong volume effects in all quantities for box lengths below $L = 1.8$ fm. For the pion these effects are somewhat larger in the wave function than in its pole mass. As a consequence the effects in the pion decay constant f_π are also larger than in the pion mass. In the region above $L = 2$ fm we find volume effects with opposite sign than the ones determined by chiral perturbation theory. Whereas chiral perturbation theory predicts an increase of the pion mass we find a slight decrease for $L = (2 - 4)$ fm with the increase setting in only below $L = 2$ fm. In the quenched theory this behaviour is in qualitative agreement with results from lattice QCD [8]. For the unquenched theory, however, the persistence of this effect in contrast to chiral perturbation theory points towards deficiencies in our truncation scheme. We expect this problem to be cured by taking into account explicit volume effects in the quark-gluon vertex along the lines of recent work on the infinite volume case [30, 38]. This will be the subject of future work.

Acknowledgments

We are grateful to Jens Braun, Bertram Klein, Jens Mueller and Jan Pawłowski for helpful discussions. This work has been supported by the

Helmholtz-University Young Investigator Grant No. VH-NG-332, and by the Helmholtz Interna-

tional Center for FAIR within the LOEWE program of the State of Hesse.

-
- [1] H. Leutwyler and A. V. Smilga, Phys. Rev. D **46**, 5607 (1992).
 - [2] E. V. Shuryak and J. J. M. Verbaarschot, Nucl. Phys. A **560** (1993) 306 [arXiv:hep-th/9212088].
 - [3] J. J. M. Verbaarschot and I. Zahed, Phys. Rev. Lett. **70** (1993) 3852 [arXiv:hep-th/9303012]; J. J. M. Verbaarschot, Nucl. Phys. B **426** (1994) 559 [arXiv:hep-th/9401092]; J. J. M. Verbaarschot, Phys. Lett. B **329** (1994) 351 [arXiv:hep-th/9402008].
 - [4] G. Akemann, P. H. Damgaard, U. Magnea and S. Nishigaki, Nucl. Phys. B **487**, 721 (1997) [arXiv:hep-th/9609174].
 - [5] J. J. M. Verbaarschot, arXiv:0910.4134 [hep-th].
 - [6] S. Aoki, T. Umemura, M. Fukugita, N. Ishizuka, H. Mino, M. Okawa and A. Ukawa, Phys. Rev. D **50**, 486 (1994).
 - [7] P. H. Damgaard, R. G. Edwards, U. M. Heller and R. Narayanan, Phys. Rev. D **61**, 094503 (2000) [arXiv:hep-lat/9907016].
 - [8] M. Guagnelli, K. Jansen, F. Palombi, R. Petronzio, A. Shindler and I. Wetzorke [Zeuthen-Rome (ZeRo) Collaboration], Phys. Lett. B **597** (2004) 216 [arXiv:hep-lat/0403009].
 - [9] B. Orth, T. Lippert and K. Schilling, Phys. Rev. D **72**, 014503 (2005) [arXiv:hep-lat/0503016].
 - [10] H. Fukaya *et al.* [JLQCD Collaboration], Phys. Rev. Lett. **98**, 172001 (2007) [arXiv:hep-lat/0702003].
 - [11] S. Necco, PoS CONFINEMENT8, 024 (2008) [arXiv:0901.4257 [hep-lat]].
 - [12] J. Gasser and H. Leutwyler, Phys. Lett. B **184** (1987) 83; J. Gasser and H. Leutwyler, Phys. Lett. B **188** (1987) 477; J. Gasser and H. Leutwyler, Nucl. Phys. B **307** (1988) 763.
 - [13] G. Colangelo, S. Durr and C. Haefeli, Nucl. Phys. B **721** (2005) 136 [arXiv:hep-lat/0503014].
 - [14] P. H. Damgaard and H. Fukaya, JHEP **0901**, 052 (2009) [arXiv:0812.2797 [hep-lat]].
 - [15] J. Berges, D. U. Jungnickel and C. Wetterich, Phys. Rev. D **59**, 034010 (1999) [arXiv:hep-ph/9705474].
 - [16] J. Braun, B. Klein and H. J. Pirner, Phys. Rev. D **71**, 014032 (2005) [arXiv:hep-ph/0408116].
 - [17] J. Braun, B. Klein and H. J. Pirner, Phys. Rev. D **72**, 034017 (2005) [arXiv:hep-ph/0504127].
 - [18] R. Alkofer, C. S. Fischer and R. Williams, Eur. Phys. J. A **38** (2008) 53 [arXiv:0804.3478 [hep-ph]].
 - [19] C. S. Fischer and R. Williams, Phys. Rev. D **78**, 074006 (2008) [arXiv:0808.3372 [hep-ph]].
 - [20] C. S. Fischer, R. Alkofer and H. Reinhardt, Phys. Rev. D **65**, 094008 (2002) [arXiv:hep-ph/0202195].
 - [21] C. S. Fischer, B. Gruter and R. Alkofer, Annals Phys. **321** (2006) 1918 [arXiv:hep-ph/0506053].
 - [22] C. S. Fischer, A. Maas, J. M. Pawłowski and L. von Smekal, Annals Phys. **322**, 2916 (2007) [arXiv:hep-ph/0701050].
 - [23] C. S. Fischer, A. Maas and J. M. Pawłowski, Annals Phys. **324**, 2408 (2009) [arXiv:0810.1987 [hep-ph]].
 - [24] C. S. Fischer and M. R. Pennington, Phys. Rev. D **73** (2006) 034029 [arXiv:hep-ph/0512233].
 - [25] C. S. Fischer and M. R. Pennington, Eur. Phys. J. A **31** (2007) 746 [arXiv:hep-ph/0701123].
 - [26] C. S. Fischer, Phys. Rev. Lett. **103**, 052003 (2009) [arXiv:0904.2700 [hep-ph]].
 - [27] T. Goecke, C. S. Fischer and R. Williams, Phys. Rev. B **79** (2009) 064513 [arXiv:0811.1887 [hep-ph]].
 - [28] P. Maris, C. D. Roberts and P. C. Tandy, Phys. Lett. B **420** (1998) 267 [arXiv:nucl-th/9707003].
 - [29] N. Nakanishi, Phys. Rev. **138** (1965) B1182.
 - [30] C. S. Fischer and R. Williams, Phys. Rev. Lett. **103**, 122001 (2009) [arXiv:0905.2291 [hep-ph]].
 - [31] A. C. Aguilar, D. Binosi and J. Papavassiliou, Phys. Rev. D **78**, 025010 (2008) [arXiv:0802.1870 [hep-ph]].
 - [32] D. Dudal, S. P. Sorella, N. Vandersickel and H. Verschelde, Phys. Rev. D **77** (2008) 071501 [arXiv:0711.4496 [hep-th]].
 - [33] Ph. Boucaud, J. P. Leroy, A. L. Yaouanc, J. Micheli, O. Pene and J. Rodriguez-Quintero, JHEP **0806**, 012 (2008) [arXiv:0801.2721 [hep-ph]].
 - [34] A. Maas, arXiv:0907.5185 [hep-lat].
 - [35] R. Alkofer, W. Detmold, C. S. Fischer and P. Maris, Phys. Rev. D **70** (2004) 014014 [arXiv:hep-ph/0309077].
 - [36] D. Zwanziger, Phys. Rev. D **65**, 094039 (2002) [arXiv:hep-th/0109224].
 - [37] C. Lerche and L. von Smekal, Phys. Rev. D **65**, 125006 (2002) [arXiv:hep-ph/0202194].
 - [38] R. Alkofer, C. S. Fischer, F. J. Llanes-Estrada and K. Schwenzer, Annals Phys. **324** (2009) 106 [arXiv:0804.3042 [hep-ph]].